Proceedings of the 4th International Congress APMAS2014, April 24-27, 2014, Fethiye, Turkey

Effect of Co_3O_4 on the Fracture Toughness and Microstructure of Yttria-Stabilized Cubic Zirconia (8YSZ)

B. Aktas[a,*] and S. Tekeli[b]

[a]Harran University, Engineering Faculty, Mechanical Engineering Department, 63300, Sanliurfa, Turkey

[b]Gazi University, Technology Faculty, Metallurgical and Materials Engineering Department, 06500, Ankara, Turkey

The effects of the addition of Co_3O_4 to yttria-stabilized zirconia (8YSZ) on fracture toughness and microstructure was investigated using micro-indentation and scanning electron microscopy (SEM). Undoped and 1–15 wt.% Co_3O_4-doped 8YSZ powders were prepared using a colloidal process and then pelletized under a pressure of 200 MPa. The 8YSZ specimens were sintered at 1400 °C for 1 h. SEM results showed that Co_3O_4 precipitated as a secondary phase among the primary 8YSZ grains. Furthermore, because of the presence of Co_3O_4 secondary phases at the grain boundaries of 8YSZ, the grain sizes of the 8YSZ samples increased with the addition of 1–15 wt.% Co_3O_4. The fracture toughness values of the undoped and 1 wt.% Co_3O_4-doped 8YSZ were determined to be 1.64 and 2.86 MPa $m^{1/2}$, respectively, indicating the fracture toughness of 8YSZ increased in 1 wt.% Co_3O_4 addition. The fracture toughness of 8YSZ increased upon the addition of 1 wt.% Co_3O_4.

DOI: 10.12693/APhysPolA.127.1384

PACS: 81.05.Je, 81.20.Ev, 81.40.Np, 82.47.Ed

1. Introduction

A fuel cell is an electrochemical device in which the chemical energy of fuel is converted into electricity through the electrochemical oxidation of the fuel. Fuel cells typically have a pair of electrodes (an anode and a cathode) and an electrolyte. The working principal of a fuel cell is similar to that of a battery. However, unlike a battery, a fuel cell does not run down or require recharging. A fuel cell operates as long as both fuel and an oxidant are supplied to the electrodes [1]. Various types of fuel cells (proton exchange membrane fuel cells, molten carbonate fuel cells, phosphoric acid fuel cells, solid oxide fuel cells, etc.) have been developed as power sources for a large number of applications. Solid oxide fuel cells (SOFCs) offer several advantages over other types of fuel cells, such as high efficiency, low emission, high power density and fuel flexibility. SOFCs are being used in various applications in the automobile, power generation, and aeronautics industries.

Zirconia can exist in three different crystal structures, monoclinic, tetragonal, and cubic, depending on the temperature and amount of the stabilizer used in production. Of the zirconia phases, yttria-stabilized cubic zirconia (8YSZ) has a fluorite structure and is well known as a solid electrolyte that possesses high oxygen ion conductivity and chemical stability over wide ranges of temperature and oxygen partial pressure. Thus, it is widely used as an oxygen sensor, a thermal barrier, and an SOFC electrolyte.

8YSZ is known to experience severe grain growth and has a high coefficient of thermal expansion, low thermal shock resistance, and poor mechanical properties (such as low fracture strength and toughness) at high operating temperatures (8YSZ electrolyte exhibits good conductivity at approximately 1000 °C, but such high operating temperatures lead to lower working efficiencies). To be useful in applications, 8YSZ should not only have high conductivity, but should also have better mechanical, chemical, and electrical stabilities at high operating temperatures. To be used as an electrolytic component of an SOFC, a material must possess both high strength and high oxygen ion conductivity at high temperatures [2, 3]. Consequently, the preparation of a high strength and high conductivity 8YSZ electrolyte is crucial. For SOFC applications, thin, solid electrolytes must be sufficiently strong and tough to withstand room temperature assembly stresses and mechanically stable to survive long periods at high temperatures, in reducing and oxidizing atmospheres. Therefore, enhancement of the mechanical properties of 8YSZ is a significant goal. Many approaches have been taken to enhance the mechanical strength and hinder the severe grain growth of 8YSZ without deteriorating its high ionic conductivity. One such approach, used in the present investigation, is to dope 8YSZ with different metal oxides and other ceramic components. When doping 8YSZ, it is known that using matrix and second phase particles with highly mismatched lattice parameters and thermal expansion coefficients inhibits grain growth, and thus, enhances room temperature mechanical properties [4].

The aim of the present study is to determine the effect of Co_3O_4 doping on the mechanical properties of 8YSZ. To accomplish this, the microstructures and fracture toughness of 1–15 wt.% Co_3O_4-doped 8YSZ samples were investigated using SEM, and micro-hardness tests.

*corresponding author; e-mail: baktas@harran.edu.tr

2. Experimental materials and procedure

The matrix material used was 8 mol.% yttria-stabilized cubic zirconia (8YSZ) (Tosoh, Japan), while Co_3O_4 powder (US Research Nanomaterials, Inc., USA), up to 15 wt.%, was used as the additive. The average grain sizes of the powders were 0.3 and 0.2 μm for 8YSZ and Co_3O_4, respectively.

The specimens used for the microstructural and mechanical investigations were produced by means of colloidal processing. Doping was carried out in a plastic container by mechanically mixing up to 15 wt.% of Co_3O_4 with 8YSZ using zirconia balls and ethanol. Mechanical mixing was performed in a "speks" type mixer at 200 rpm for 12 h. Following mixing, the container lid was removed and the prepared slurry was left to air dry for 24 h. After drying, the medium hardness agglomerated powders were ball milled for 10 min to obtain good dispersions and to break-up agglomerates. The powders were then passed through a 60 μm sieve and pressed at 40 MPa in a single-axis die with a radius of 10 mm and a height of 4 mm. The inner surface of the steel die was cleaned after each dry pressing, and stearic acid was applied to its side walls. Sintering was carried out in a box-type furnace under normal atmospheric conditions. The pressed pellets were pre-sintered at 1000 °C and then sintered at 1400 °C for 1 h. Heating and cooling were carried out at a rate of 5 °C/min. The surfaces of the sintered specimens were ground and polished using a normal metallographic method after the sintering process, and then thermally etched at 1350 °C for 1 h. Microstructural investigations of the sintered specimens were performed using a scanning electron microscope (SEM, JEOL LV 6060). The grain sizes of the specimens were measured using the mean linear intercept method. In addition, the average grain sizes of the specimens were determined using the following equation:

$$D = \frac{L_i}{N_i M}, \tag{1}$$

where L_i is the length of the line, N_i is the number of grain-boundary intercepts, and M is the magnification in the photomicrograph of the material.

Both the hardness and fracture toughness of the specimens were determined using a Vickers hardness tester using a load of 2 kg and duration of 15 s. Hardness values were calculated using the following equation:

$$H_v = \frac{1854P}{d^2}, \tag{2}$$

where $H_V P$ is the applied load (kg) and d is the mean value of the diagonal length (mm). Fracture toughness values were calculated by measuring the length of the cracks that formed at the edges of the track that resulted from the hardness tests. Cracks were measured immediately after applying the load to the specimen so that they would not be affected by environmental factors. Fracture toughness was calculated using the "half-penny-crack" formula proposed by Anstis *et al.* [5]:

$$K_{IC} = 0.016 \left(\frac{E}{H_V}\right)^{\frac{1}{2}} \left(\frac{P}{C^{\frac{3}{2}}}\right)^{\frac{1}{2}}, \tag{3}$$

where E is Young's modulus, H_V is the Vickers hardness, P is the applied load, and C is the crack length.

3. Experimental results and dicussion

The post-sintering microstructures of the specimens doped with various amounts of Co_3O_4 are presented in Fig. 1. The SEM micrographs of the 5, 10, and 15 wt.% Co_3O_4-doped 8YSZ samples indicate that Co_3O_4 precipitated as a secondary phase among the primary 8YSZ grains (Fig. 1c-1e). The reason for this is that the Co_3O_4 did not fully dissolve in the 8YSZ, and thus, it precipitated at triple-points and along grain boundaries. Additionally, the microstructure of the undoped 8YSZ shows that it is composed of fine coaxial polygonal grains (Fig. 1a) and the microstructures of Co_3O_4-doped 8YSZ samples show coarse-grained structures (Fig. 1b-1e).

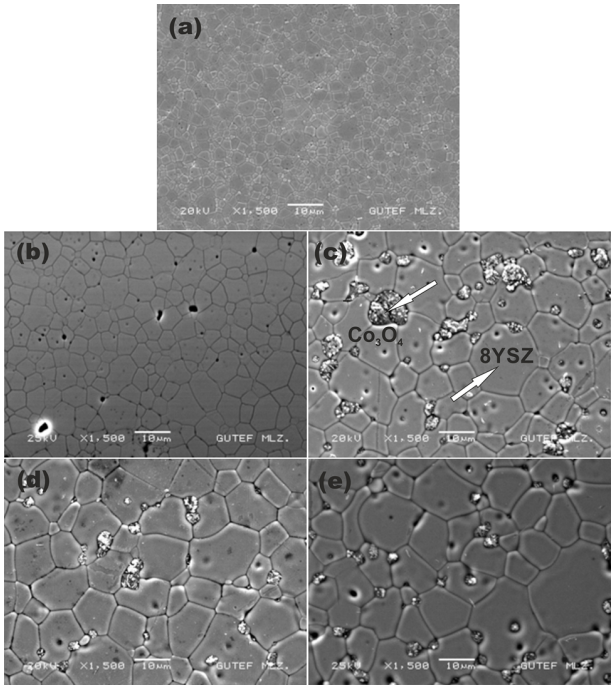

Fig. 1. Microstructures of undoped and Co_3O_4-doped 8YSZ specimens sintered at 1400 °C for 1 h. (a) Undoped 8YSZ, (b) 1 wt.% Co_3O_4-doped 8YSZ, (c) 5 wt.% Co_3O_4-doped 8YSZ, (d) 10 wt.% Co_3O_4-doped 8YSZ, and (e) 15 wt.% Co_3O_4-doped 8YSZ.

Figure 2 shows how grain size of 8YSZ changes with Co_3O_4 content. From this figure, it can be seen that average grain size increases with Co_3O_4content. These grain boundary phases may increase grain boundary mobility, thus leading to increased grain growth. It has been previously reported that Co_3O_4-doped samples exhibit high grain growth rates in the final stage of sintering, likely due to the gradual loss of pore drag on grain boundary migration [6].

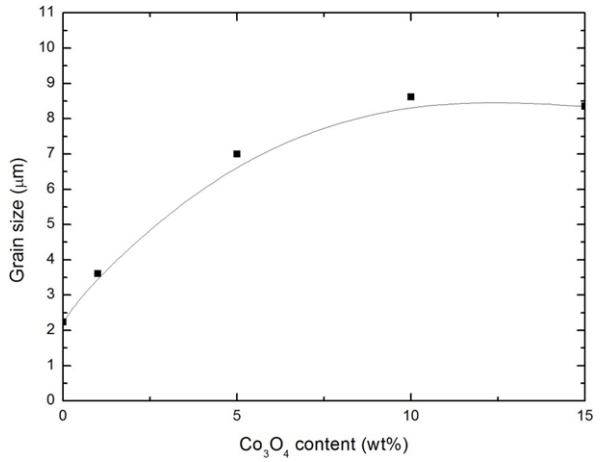

Fig. 2. Plot of grain size versus Co_3O_4 content of the doped and undoped 8YSZ specimens after sintering at 1400 °C for 1 h.

The post-sintering hardness and fracture toughness of the 8YSZ specimens doped with various amounts of Co_3O_4 are shown in Fig. 3. The hardness and fracture toughness tests were performed using a Micro-Vickers hardness testing machine using a load of 2 kg and a dwell time of 15 s. The hardness of a ceramic is usually affected by its intrinsic deformability and microstructural features, such as multiphases, grain size, orientation, porosity, and grain boundary composition [7]. The addition of 1 wt.% Co_3O_4caused a slight decrease in the hardness of 8YSZ, whereas additions of 5, 10, and 15 wt.% Co_3O_4 increased hardness. It had been reported that the solubility limit of Co_3O_4 in 8YSZ is 1 wt.% [8]. Co_3O_4 has a lower hardness than 8YSZ [9]. Thus, it was thought that 1 wt.% Co_3O_4 would reduce the hardness of 8YSZ. However, over-doped Co_3O_4 (i.e., 5, 10, and 15 wt.% Co_3O_4) precipitated as a secondary phase at the grain boundaries of 8YSZ. The presence of secondary phases at grain boundaries may be the cause of the increased hardness of 8YSZ.

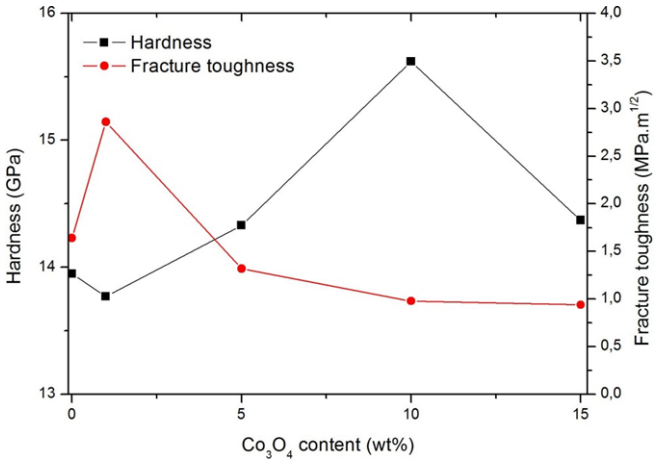

Fig. 3. Effects of Co_3O_4 content on the hardness and fracture toughness of 8YSZ samples sintered at 1400 °C for 1 h.

The fracture toughness values of the undoped and 1 wt.% Co_3O_4-doped 8YSZ specimens were calculated to be 1.64 and 2.86 MPa m$^{1/2}$, respectively. The fracture toughness of 8YSZ increased as a result of the addition of 1 wt.% Co_3O_4; however, it diminished when 5, 10, and 15 wt.% were added (Fig. 3). The increase in fracture toughness observed after the addition of 1 wt.% Co_3O_4 can be explained in terms of crack deflection at the crack tip and bridging of the process zone by the second phase. As seen in the SEM micrograph of the 1 wt.% Co_3O_4 sample, shown in Fig. 1b, a thin glassy phase occurred at the grain boundaries of 8YSZ. These secondary glassy phases might deflect cracks and this crack deflection could be the reason for the observed improvement in fracture toughness with addition of 1 wt.%. Furthermore, from fracture toughness analyses showed drastic decreases in values after over-additions of Co_3O_4 (i.e., 5, 10, and 15 wt.%). The decreased fracture toughness values may be due to the formation of grains within the Co_3O_4-overdoped 8YSZ samples, resulting in decreased total grain boundary volumes in overdoped 8YSZ samples.

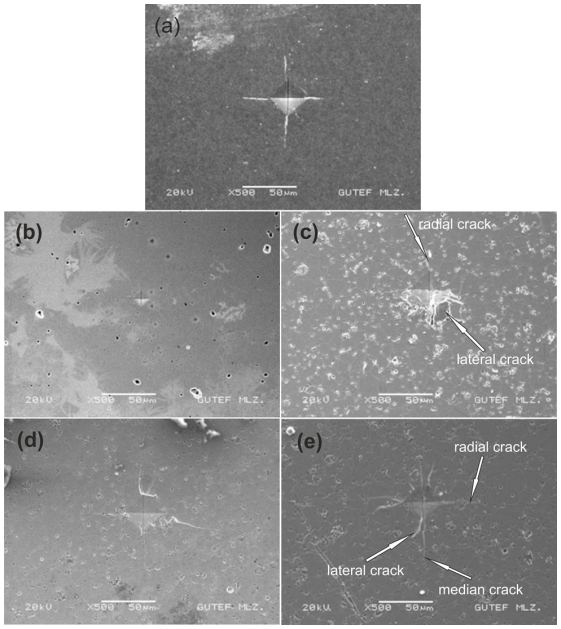

Fig. 4. SEM micrographs of Vickers indentations with different crack lengths. (a) Undoped 8YSZ, (b) 1 wt.% Co_3O_4-doped 8YSZ, (c) 5 wt.% Co_3O_4-doped 8YSZ, (d) 10 wt.% Co_3O_4-doped 8YSZ and (e) 15 wt.%-Co_3O_4 doped 8YSZ.

Figure 4 shows SEM micrographs of cracks generated by an indentation load of 2 kg, applied for 15 s. Cracks can be seen at the corners of the indentations of all samples (Fig. 4a-4e). It should be noted that the cracks emanated from the corners of the indents and that crack lengths differed according to Co_3O_4 content. Undoped and Co_3O_4-doped 8YSZ specimens exhibited four kinds of cracks: median, radial, palmqvist, and lateral. Median and radial cracks were generally observed in undoped 8YSZ (Fig. 4a). Palmqvist and lateral cracks,

however, were observed in the Co_3O_4-doped 8YSZ specimens (Fig. 4b-4e).

4. Conclusions

The addition of Co_3O_4 to 8YSZ increased the average grain size. The grain size of 8YSZ changed from 2.24 μm to 8.35 μm with the addition of Co_3O_4. The over-addition of Co_3O_4 (i.e., 5, 10, and 15 wt.%), which is especially insoluble in 8YSZ, formed a secondary phase among the primary 8YSZ grains. Results show that the fracture toughness of 8YSZ increased from 1.64 MPa m$^{1/2}$ to 2.86 MPa m$^{1/2}$ with the addition of 1 wt.% Co_3O_4. This increase in fracture toughness is due to crack deflection, resulting from the presence of a thin glassy phase at 8YSZ grain boundaries.

Acknowledgments

This work has been supported by HUBAK (the scientific research projects commission of Harran University, Sanliurfa, TURKEY) under project number K14005. The authors are grateful to the scientific research projects commission of Harran University for financial support, and Gazi University for the provision of laboratory facilities.

References

[1] N. Bamba, Y.H. Choa, T. Sekino, K. Niihara, *J. Eur. Ceram. Soc.* **18**, 693 (1998).

[2] T. Zhang, Z. Zeng, H. Huang, P. Hing, J. Kilner, *Mater. Lett.* **57**, 124 (2002).

[3] N.H. Kwon, G.H. Kim, H.S. Song, H.L. Lee, *Mat. Sci. Eng. A-Struct.* **299**, 185 (2001).

[4] T. Chen, S. Tekeli, R.P. Dillon, M.L. Mecartney, *Ceram. Int.* **34**, 365 (2008).

[5] G.R. Anstis, P. Chantikul, B.R. Lawn, D.B. Marshall, *J. Am. Ceram. Soc.* **64**, 533 (1981).

[6] J. Li, T. Ikegami, T. Mori, *Acta Materialia* **52**, 2221 (2004).

[7] W.E. Lee, W.M. Rainforth in: *Ceramic Microstructures: Property control by processing*, London, UK: Chapman and Hall, 1994.

[8] B. Aktas, S. Tekeli, *Int. J. Mater. Res.* **105**, 577 (2014).

[9] S. Sakamoto, M. Yoshinaka, K. Hirota, O. Yamaguchi, *J. Am. Ceram. Soc.* **80**, 267 (1997).